PHOTOMASK

BACUS—The international technical group of SPIE dedicated to the advancement of photomask technology.

Zeiss Best Student Poster Winner (PUV20)

Accuracy analysis of a stand-alone EUV spectrometer for the characterization of ultrathin films and nanoscale gratings

Sophia Schröder, Lukas Bahrenberg, Nimet Kutay Eryilmaz, Sven Glabisch, and Sascha Brose, RWTH Aachen University TOS - Chair for Technology of Optical Systems, Aachen, Germany; JARA - Fundamentals of Future Information Technology, Jülich, Germany

Serhiy Danylyuk, Fraunhofer ILT - Institute for Laser Technology, Aachen, Germany

Jochen Stollenwerk and Peter Loosen, RWTH Aachen University TOS - Chair for Technology of Optical Systems, Aachen, Germany; JARA - Fundamentals of Future Information Technology, Jülich, Germany; Fraunhofer ILT - Institute for Laser Technology, Aachen, Germany

ABSTRACT

In this contribution the accuracy of measurements performed with a stand-alone EUV spectrometer is analyzed. The setup is used to determine optical constants and dimensional characteristics of samples, e.g. ultrathin films or nanoscale gratings. For this purpose, measurements of the broadband EUV reflectance of the samples at variable grazing incidence angles are used to reconstruct sample parameters in a model-based approach. The accuracy of these measurements is a crucial factor for a reliable characterization of samples. We present an overview on the sources of uncertainties in the experimental setup as well as improvements to the setup that improves its accuracy. Additionally, the reconstruction accuracy of the optical constants is analyzed. A focus is put on the influence of the experimental uncertainty and the range of incidence angles used for reflectance measurements.

1. Introduction

The semiconductor industry has pushed the size of fabricated structures well into the nanoscale regime and structures have progressively become more complex. The emergent fabrication technique of the industry, extreme ultraviolet (EUV) lithography, is continuously adapting to the corresponding fabrication challenges. Both in research and industry, there is a permanent need for improved metrology techniques to aid these

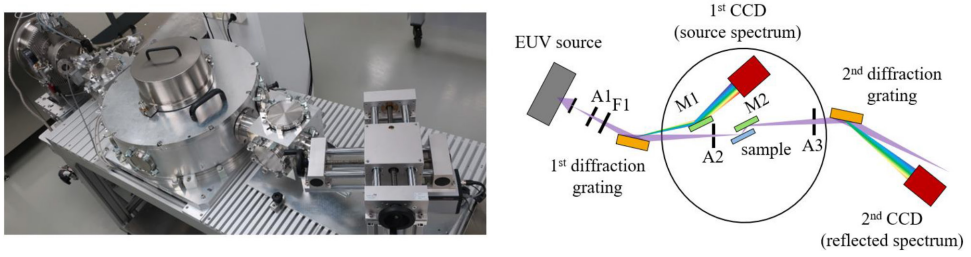

Figure 1. Left: Photograph of the stand-alone EUV spectrometer in cleanroom environment (footprint 2.5 × 1 mÇ). Right: Schematic of the experimental setup with its main components. The EUV beam is indicated in purple (abbreviations: A = apertures, F = spectral filters, M = deflection mirrors, CCD = charge-coupled device cameras).

BACUS NEWS

DECEMBER 2020
VOLUME 36, ISSUE 12

SPIE.

11517-25

EDITORIAL

What will the photomask community's new normal be?

Emily Gallagher, imec

In January of this year, I had the opportunity to select a topic worthy of a BACUS Newsletter editorial. At that time, I chose climate change and its impact on the photomask community. Today, I am again searching for a subject worthy of an editorial. I initially resisted the gravitational pull of the pandemic because its influence on our lives is already inescapable, but I cannot ignore it for that same reason. In the spirit of J.K. Rowling, I will focus on the impact of the 2020 novel virus, but not name the illness itself. Instead, consider the impact to our working lives. In 2020 the business of making masks has changed. While some need to be physically present to fabricate masks or to run the experiments to push development forward, others work entirely remotely. As a community, we have eliminated international travel and in-person meetings of all kinds. We can like it or not, but we are largely working online. We have replaced meeting rooms with Teams, Zoom or some other virtual platform. We have attended conferences virtually and tried to replicate networking with chat rooms. We are generating more masks, executing more complex data prep and inserting advanced technologies like EUV and MBMW. We are fortunate that this pandemic has given us more business opportunities, not fewer.

A recent survey from McKinsey & Company[1] quantifies the aggressive adoption of company changes because of the pandemic – it has been 20 to 25 times faster. Pace is one component, but what type of change is occurring? Does the change relate to photomask or semiconductors at all? The survey lists obvious changes like migration to remote working and adoption of advanced technologies. The survey also mentioned the emerging need for more pervasive data security and redundancies in the supply chain. For the semiconductor industry, and the photomasks on which the industry stands, this means more business volume. In many cases, these changes were planned, but the urgency of implementation changed and they became a top business priority. The largest shifts of 2020 are those most likely to stick because they mattered most during a time of upheaval. This means that we need to be intentional about the changes that are occurring now. We have an opportunity that is well articulated by Fareed Zakaria in his Washington Post article[2]:

"In most eras, history proceeds along a set path and change is difficult. But the novel coronavirus has upended society. People are disoriented. Things are already changing, and, in that atmosphere, further change becomes easier than ever."

We are a community of photomask makers, working internationally on all aspects of masks from research, to fabrication, to sales and all the associated infrastructure. This is our chance to consider the industry and our roles holistically. Does working from home and its inherent efficiencies in office space and time make sense for us? Do we need to change our shipping logistics when there are fewer people in the manufacturing sites? Do we really need to travel globally to enable meaningful business and technical reviews? How can we ensure that attendees really commit to virtual events like conferences if they are here to stay? What do you want to implement in 2021 now that change is easier?

---

1. LaBerge, Laura, et al., (2020, October 5) "How COVID-19 has pushed companies over the technology tipping point – and transformed business forever". https://www.mckinsey.com/business-functions/strategy-and-corporate-finance/our-insights/. Accessed 20 Nov 2020.
2. Zakaria, Fareed "The pandemic upended the present. But it's given us a chance to remake the future." Washington Post, 16 Oct. 2020, https://www.washingtonpost.com/opinions/2020/10/06/fareed-zakaria-lessons-post-pandemic-world. Accessed 20 Nov 2020.

BACUS

N • E • W • S

BACUS News is published monthly by SPIE for *BACUS*, the international technical group of SPIE dedicated to the advancement of photomask technology.

Managing Editor/Graphics Linda DeLano
SPIE Sales Representative, Exhibitions, and Sponsorships Melissa Valum
BACUS Technical Group Manager Marilyn Gorsuch

SPIE.

P.O. Box 10, Bellingham, WA 98227-0010 USA
Tel: +1 360 676 3290
Fax: +1 360 647 1445
SPIE.org
help@spie.org

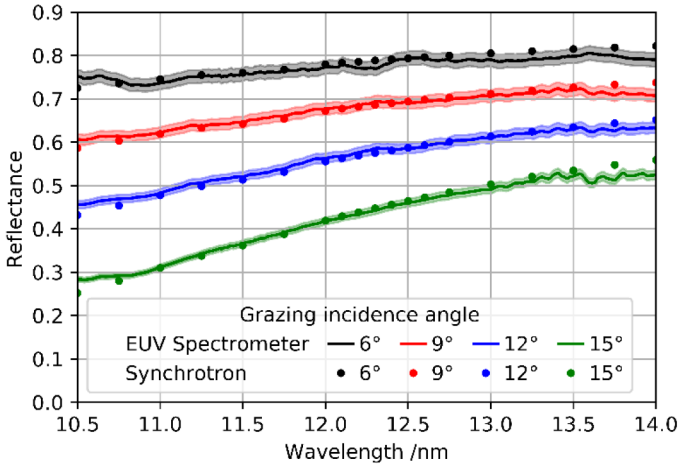

Figure 2. Benchmarking of measurement accuracy of the stand-alone EUV spectrometer to synchrotron measurements at PTB, Berlin.

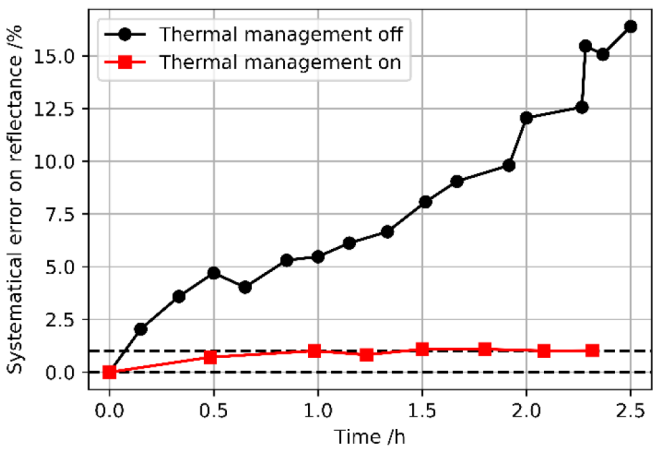

Figure 3. Thermal instability of the first CCD camera with and without thermal management.

developments and allow for quality control of device fabrication while satisfying the accuracy requirements of the semiconductor industry[1, 2].

Metrology techniques used currently in the semiconductor industry are non-imaging techniques like scatterometry[3]. These techniques are non-destructive and fast. Their resolution and sensitivity to sample parameters is dependent on the utilized wavelength regime. Here, the utilization of EUV radiation offers a great number of advantages which were summarized in previous pulications[4, 5]. Currently EUV scatterometry is usually conducted at synchrotron facilities, which deliver highly accurate measurements, but the maintenance of the synchrotrons is costly. Additionally, measurements are only conductible at the facility, which make it not applicable for in-line quality control of device fabrication.

Grazing incidence EUV spectrometry with a stand-alone EUV spectrometer is a promising metrology technique for applications in the semiconductor industry. In this non-imaging technique, the broadband EUV reflectance of samples is measured at varying grazing incidence angles. From the acquired data, sample parameters are reconstructed in a model-based approach. Several applications of EUV spectrometry with the stand-alone setup realized at RWTH Aachen University have been already presented in previous publications. This includes the characterization of ultrathin film systems regarding their geometrical layer structure and material composition[6], the determination of the optical constants of novel materials in the EUV spectral range[5] and critical dimension metrology of nanoscale gratings[7].

When suggesting the stand-alone EUV spectrometer for industrial measurement tasks, a key factor that must be considered is the accuracy of the parameter reconstruction. The reconstruction accuracy for the different applications is dependent on three main factors: the experimental accuracy of the reflectance measurement conducted with the EUV spectrometer, secondly the number of meaningful data points acquired during measurements and thirdly the accuracy of the model used for parameter reconstruction. Within the scope of this work the experimental accuracy is determined and measures to enhance the accuracy are proposed. Furthermore, the reconstruction accuracy is investigated, where three main factors are identifiable. In this work the sole influence of the experimental accuracy and the number of meaningful data points is determined, while the influence of the model accuracy was suppressed. In future work the model accuracy will be investigated separately.

2. EUV Spectrometer

The stand-alone EUV spectrometer developed at RWTH Aachen University has already been part of previous publications[5, 6]. Nonetheless, the setup and measurement procedure are briefly explained in this chapter to provide a basic understanding for the following experimental accuracy analysis. The overall setup consists of several connected vacuum chambers and uses a compact discharge produced plasma (DPP) EUV source[8]. Two sequential spectrographs are placed in the vacuum chambers to measure the broadband reflectance of a sample in the EUV spectral range. Grazing incidence angles can be varied in the range from 5° to 15°. As a result, a set of reflectance curves is extracted that serve as a basis for the sample parameter reconstruction. A picture and schematic representation of the setup is shown in figure 1.

The DPP source produces a plasma pinch of ~ 400µm diameter and is operated at a repetition rate of 50 Hz. The relative spectral distribution of EUV radiation is adjustable by the selection of working gases and the discharge voltage. By placing an entrance slit with 50µm width in close vicinity to the plasma pinch, the beam width in horizontal direction is defined. For spectral out-of-band filtering, a 200nm thick zirconium filter is placed at position A1. Additional transmission filters for intensity or bandwidth tuning can be placed at position F1.

Both spectrographs are flat field spectrographs with curved diffraction gratings. The curved gratings have an imaging property along the horizontal axis which images the entrance slit onto the sample or the charge-coupled device (CCD) camera. The first spectrograph is illuminated by the entrance slit. While the first diffraction order is directed onto the first CCD camera to capture the source spectrum, the zeroth diffraction order is focused onto the sample. After interaction with the sample, the second spectrograph is used to measure the first diffraction order on the second CCD camera capturing the reflected spectrum. The deflection mirrors M1 and M2 are used to guide the beam trajectory and apertures at position A2 and A3 are used to reduce straylight. All components are aligned with the use of several alignment cameras, additionally to the two mentioned CCD camera.

Detection of the EUV spectra is conducted by two two-dimensional CCD cameras. Both cameras utilize a back thinned CCD sensor for EUV detection with a sensor area of 512 × 2048 pixels and a pixel size of 13.5µm × 13.5µm. In both, vertical and horizontal direction, the whole spectral image is captured by the CCD sensors and can be measured in a single measurement.

For the determination of the absolute reflectance of a sample, the influence of the optical setup must be taken into account. Each optical component influences the intensity level and distribution of the radiation due to its distinctive reflectance, absorption or beam cutting character. To account for these effects, a calibration of the setup is conducted with a sample of known reflectance which has been characterized at a synchrotron in advance. As a result, the influence of all components is summarized in a tool factor, which is taken into account when determining the absolute reflectance of a sample.

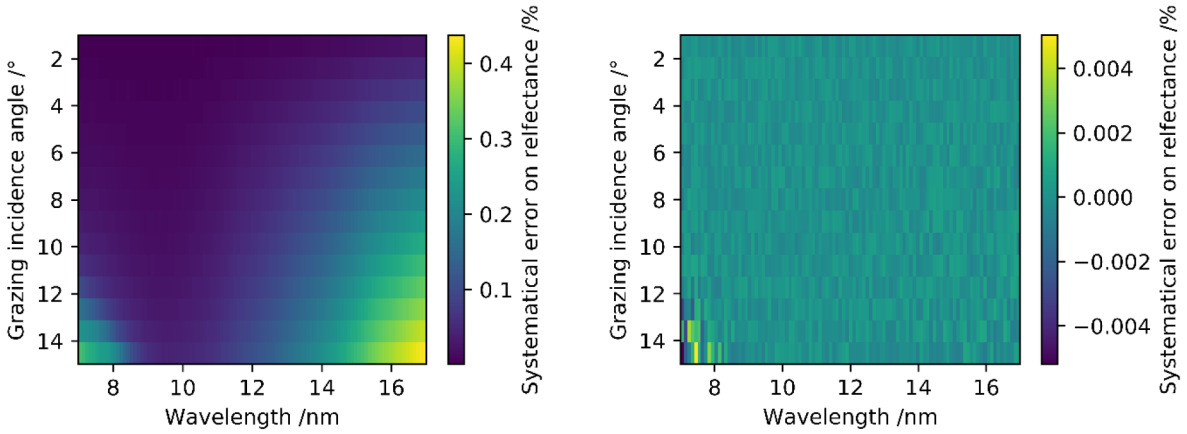

Figure 4. Left: Systematical error on the reflectance measurement induced by a polarization offset between non-polarized radiation and a combination of 49% p-polarized and 51% s-polarized radiation. Right: Systematical error on the reflectance measurement induced by assuming calibration measurement is done with perfectly monochromatic radiation instead of radiation with 0.02nm spectral resolution.

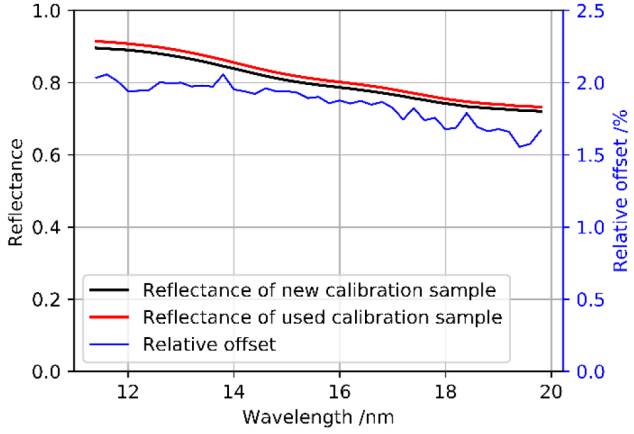

Figure 5. Reflectance of two calibration samples measured at the synchrotron of PTB, Berlin. Relative offset between both reflectance curves is shown as blue curve.

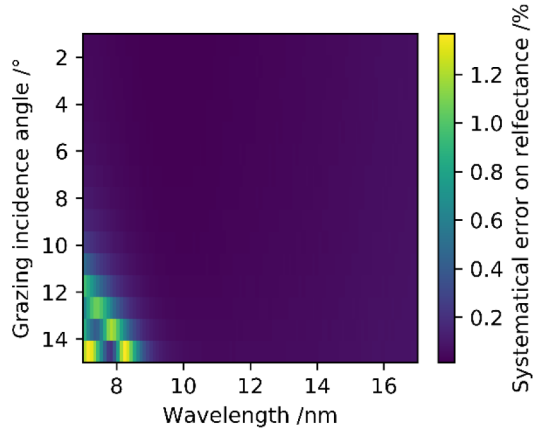

Figure 6. Systematical error on the reflectance measurement induced by an angular alignment offset between calibration sample and sample under investigation of 0.01°.

3. Experimental Accuracy Analysis

The stand-alone EUV spectrometer is a vacuum-based setup consisting of a multitude of optical and other components. Every hardware component influences the experimental accuracy of the measurements. The experimental accuracy is quantitively expressed in form of uncertainties on the measurement result[9]. In previous works the relative uncertainty of the reflectance measurements with the EUV spectrometer was assumed to be ~2%, which is supported by benchmarking experiments that compare the reflectance of samples measured with the stand-alone spectrometer data to measurements conducted at the synchrotron facility of Physikalisch-Technische Bundesanstalt (PTB) in Berlin. As can be seen in figure 2, for the measured wavelength interval from 10.5nm to 14nm both datasets are in good agreement within their uncertainties.

The uncertainty of a measurement is a measure for the possible deviations between measured result and true value[9]. These deviations are called errors and are either of statistical or systematical nature. Statistical errors are statistically fluctuating deviations, that change with every measurement. Systematical errors are constant offsets of the measured value from the true value. Statistical errors are reduced by repeating a measurement and averaging the results. Systematical errors on the other hand cannot be reduced by multiple measurements. Still, some systematical errors can be detected and corrected using correction terms. The remaining ones can be treated as an additional unknown measurement parameter during the parameter reconstruction.

Errors are caused by a broad number of sources including every component in the setup and measurement method. These errors can be ascribed either to the measurement result itself or the measurement parameters. In the following a distinction is drawn between errors on the reflectance measurement and errors on the two measurement parameters, the incidence angle and wavelength.

3.1 Experimental reflectance accuracy

In this section a number of error sources is listed, which were identified in the scope this work.

EUV Source To the EUV Source only a statistical error is attributable. The radiating plasma pulses of the EUV source are not stable in intensity from pulse to pulse[10]. To track the fluctuations during a measurement the source spectrum is recorded simultaneously with the reflected spectrum of the sample, which reduces the error induced by the fluctuations.

CCD Cameras

The second identifiable source of statistical errors in the setup is the signal processing of the two CCD cameras. Measurements with CCD cameras consist of two measurements: the dark signal measurement and the signal measurement. The dark signal is detected when the EUV beam is blocked by an electrical shutter. It captures the dark current of the CCD camera as well as permanent straylight and other artefacts of the CCD camera. Both measurements suffer from detection noise which is a combination of several intrinsic effects of the CCD camera like photon shot noise and

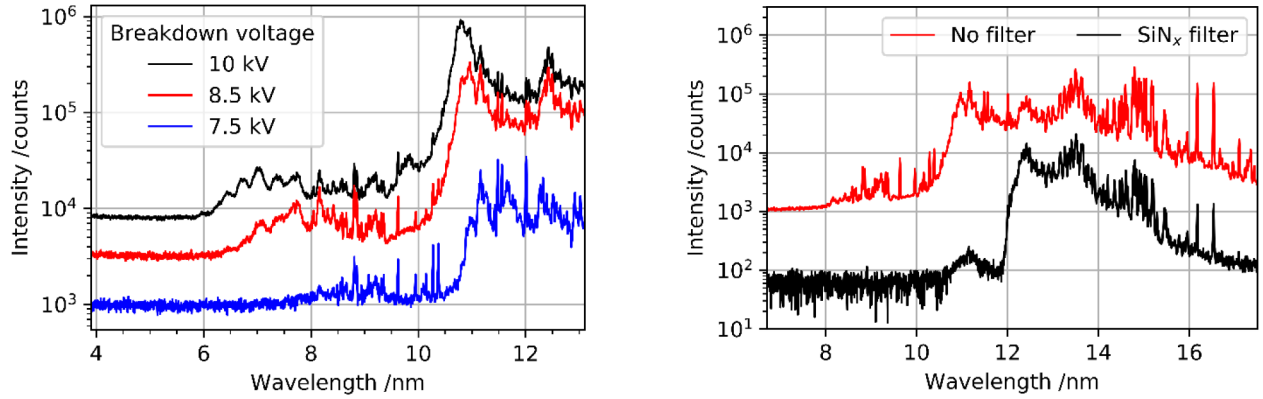

Figure 7. Left: Spectral intensity distribution of the EUV radiation for different breakdown voltages of the DPP source. The signal below 6nm is estimated to be induced by straylight. Right: Measurements of the EUV spectrum from ~8nm to 17.5nm, once with and once without a 200nm thick spectral filter of silicon-rich nitride.

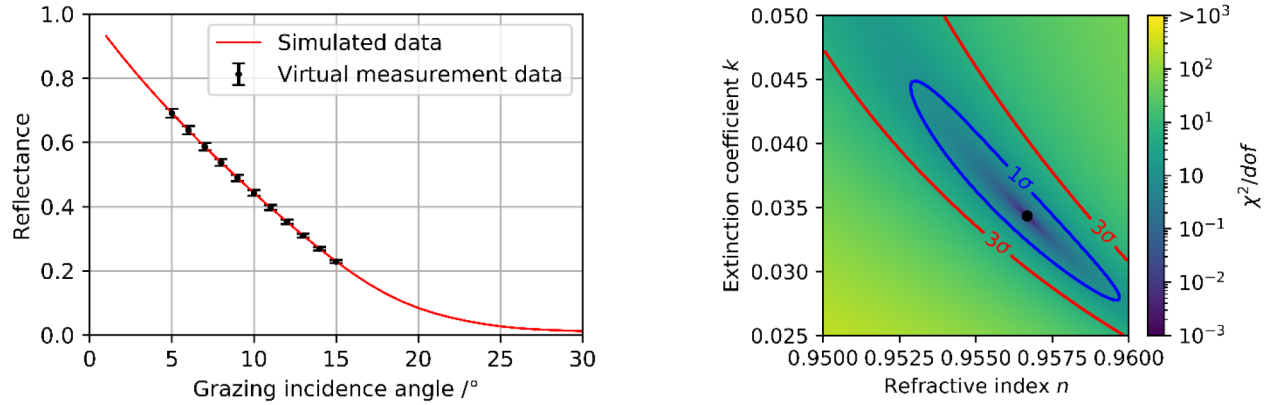

Figure 8. Left: Synthetic reflectance measurement data of a 40nm layer of tantalum on a silicon substrate at 13.5nm wavelength, dependent on the incidence angle θ with a synthetic, relative experimental uncertainty of 2%. Data for the optical constants of the materials were taken from CXRO database[14]. Right: Confidence interval plots for the reconstruction of the optical constants n and k. The χ^2/dof for the fitting of simulated reflection curves is plotted for different combinations of n&k to the synthetic data set shown in the left graph. The blue and red line indicate the 1σ- and 3 σ- confidence interval, the black dot indicates the parameter combination of the best fit.

read-out noise[11]. To reduce the influence of the statistical errors, the dark signal as well as the EUV signal is measured several times and averaged. Consequently, the statistical uncertainty of a single spectral image can be reduced to be below 0.15%.

The most significant systematical error on the reflectance measurements can be ascribed to the first CCD camera which is placed completely inside the vacuum chamber of the setup (see figure 1). The measurement signal suffers from thermal instability as the electronical components of the camera heat up during measurements. In figure 3 a drift of the derived reflectance is visible over the measurement time which amounts to several percent per hour. A thermal management of the CCD camera is introduced which is a measurement routine that includes cool-down periods of the camera. Thereby, the influence on the relative measurement uncertainty is controlled to be ~1%. In future works, the thermal instability will further be reduced through an in-vacuum cooling concept for the CCD camera. This is part of ongoing work.

Setup Calibration

Every optical component in the setup, e.g. absorption filters and deflection mirrors, interacts with the EUV beam due to its optical property like the transmittance or reflectance. These properties depend on several parameters of the individual component, like the material composition, thickness or incidence angle of the EUV beam onto the surface. As all these parameters are only determinable within an uncertainty, which all would have to be considered for the experimental accuracy. To mitigate these effects the setup is calibrated with a sample of known reflectance and only a single uncertainty on the tool factor remains.

The reflectance of the calibration sample was measured at a synchrotron facility with measurement uncertainties given for the data in the order of 0.1%. As the measurement conditions at the synchrotron are not identical to the conditions at the EUV spectrometer setup, these differences must be considered during calibration of the setup. Such differences are the polarization state of the EUV radiation and the spectral resolution. The synchrotron measurements are done with p- and s-polarized radiation, while the DPP source of the spectrometer emits unpolarized radiation, which is equivalent to 50% p-polarized and 50% s-polarized radiation. In the EUV spectrometer it is slightly polarized by the optical components. The combination of s- and p-polarization of the incoming EUV beam on the sample is calculated within a relative error of below 1% and the data from the synchrotron measurements is considered accordingly. To estimate the corresponding systematical error on the reflectance measurements, the reflectance of the calibration sample is calculated once for unpolarized radiation and once for a combination of 49% p-polarized and 51% s-polarized radiation for a broad spectral and angular range. The relative offset of both reflectance data sets is plotted in the left graph of figure 4 and gives an estimation on the upper limit of the systematical error. For the wavelength range of 10.5nm to 14nm the corresponding uncertainty on the tool factor is below 0.2% and can rise up to values of 0.44% for a broader spectral range.

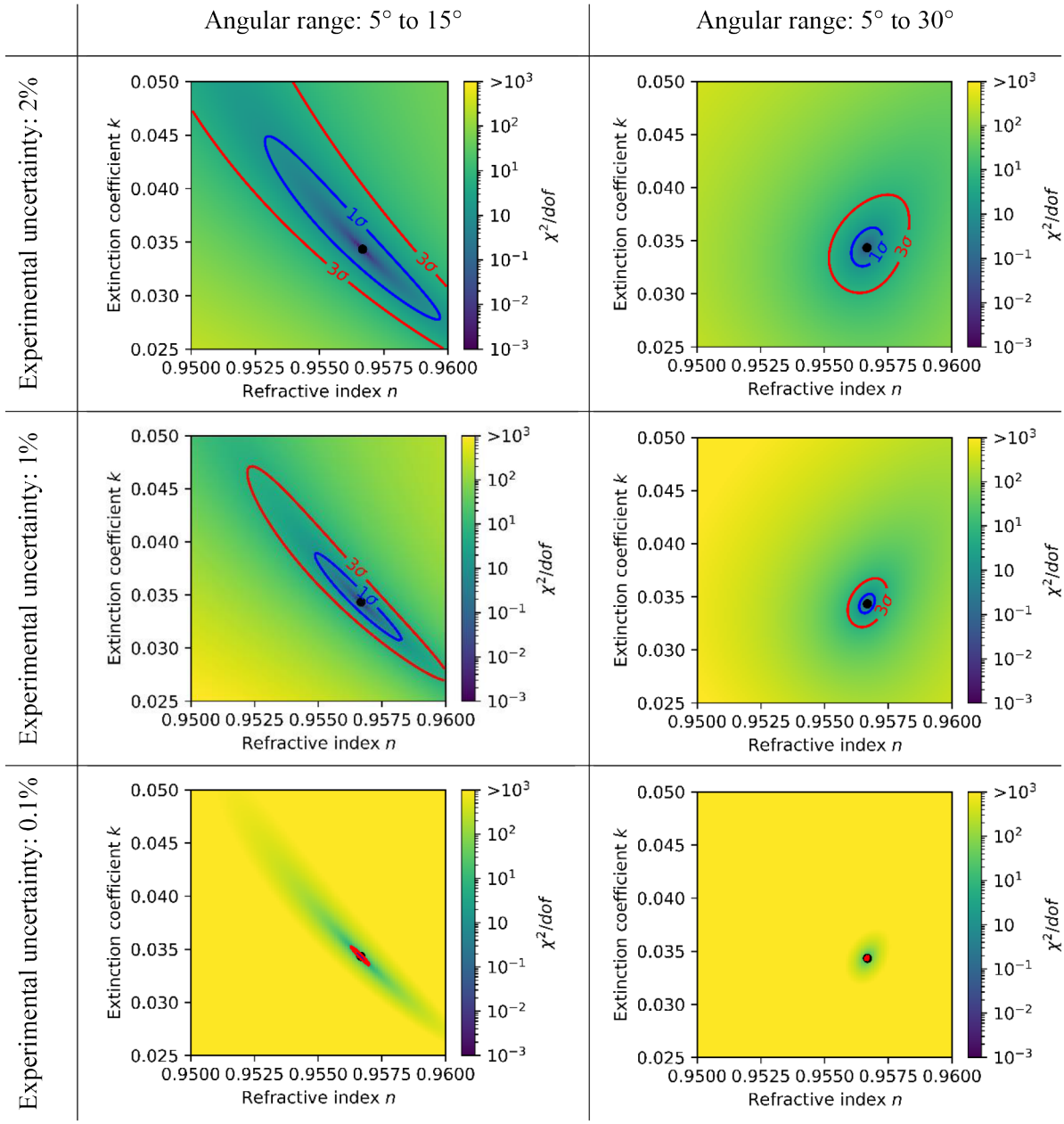

Figure 9. Confidence interval plots for the fitting of simulated reflection curves for a tantalum sample for different combinations of the optical constants n&k for three different synthetic experimental uncertainties of 2%, 1% and 0.1% from left to right respectively, and two different angular ranges, 5° to 15° on the top row and 5° to 30° on the bottom row.

The spectral resolution of the EUV spectrometer is given by the spectrograph's entrance slit width of 50μm and is determined to be ~0.02nm. The estimation on the respective systematical error on the reflectance measurement was done in the same way as for the influence of the polarization. For an upper limit on the error on the reflectance the spectral resolution of the synchrotron data was assumed to be perfectly monochromatic. Even then, the influence induced by the different spectral resolutions is determined to be below 0.005% (see figure 4 on the right). The degradation of the calibration sample has a larger influence on the experimental accuracy. As various publications show[12], samples under EUV radiation are prone to grow contamination layers on their surface, which alters their reflectance over time. To investigate the influence of the EUV-induced degradation two seemingly identical samples are measured at the synchrotron facility. The only difference between the samples is that one was not yet used as a calibration sample, while the other one was already irradiated with EUV radiation for several days. Comparing the reflectance of the two calibration samples in figure 5 show discrepancies of up to 2% in their reflectance. By using correction terms for the sample degradation, the influence on the tool factor uncertainty should reducible. In future works, the influence of sample degradation will be further reduced by using already degraded samples as calibration samples as previous investigations showed that the buildup rate of carbon contamination decreases over time[12].

The last factor to be considered with respect to the setup calibration is the alignment reproducibility between the calibration sample and the sample under investigation. An offset either in angle or position alters the beam trajectory and consequently the incidence angle and beam position on the following optical components. With the help of

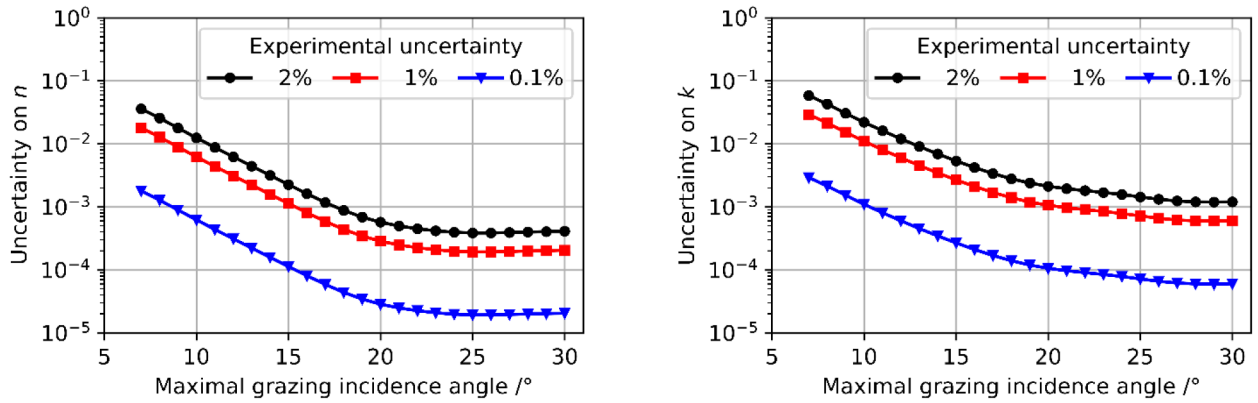

Figure 10. Reconstruction uncertainty on the refractive index n *of tantalum on the left and the extinction coefficient* k *of tantalum on the right, depending on the range of incidence angles considered during reconstruction starting at 5° for 2%, 1% and 0.1% experimental uncertainty on the reflectance measurements.*

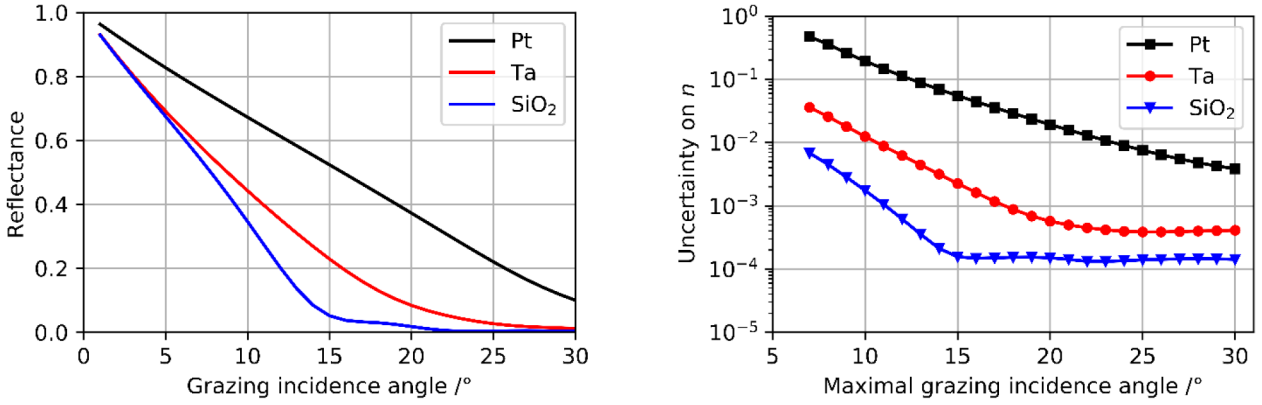

Figure 11. Left: Reflectance of silicon dioxide, platinum and tantalum at 13.5nm dependent on the grazing incidence angle. Right: Reconstruction uncertainty on the refractive index n *at 13.5nm for silicon dioxide (SiO_2), platinum (Pt) and tantalum (Ta) dependent on the range of grazing incidence angles starting at 5°.*

an alignment camera in front of the second diffraction grating (in figure 1 position A3), the beam is aligned within a beam offset of below one pixel of 13.5µm width. This offset can be ascribed to a combination of a maximum sample shift of below 6µm and a maximum angular offset of the sample of below 0.01°. While a shift of the sample does not influence the measurements in a detectable way, the alignment offset of the incidence angles gives rise to an error in the measured reflectance as can be seen in figure 6. To calculate the influence of the angular offset onto the reflectance measurements, not only the angular offset on the sample is considered but also on the subsequent optical components. For most parts of the angular and spectral range the error is in the order of ~0.01% and therefore negligible but it reaches up to ~1.5% for small wavelength below 9nm and incidence angles above 10°.

Higher diffraction orders

Another source of systematical errors in a spectrograph are higher diffraction orders of the diffraction grating which superpose the first diffraction order. The signal coming from the higher diffraction orders is not easily distinguishable from the first diffraction order. Estimations on the according influence are not trivial and rely on a correct calculation of the diffraction efficiency of the gratings. Reducing the influence of higher diffraction orders is possible by manipulating the EUV spectral range. In the EUV spectrometer filtering of radiation below 5nm is done by using the deflection mirrors M1 and M2 (figure 1), which both are irradiated at least under 5° and the zirconium filter of 200µm at position A1. Additionally, the spectral range of the EUV radiation emitted by the EUV source can be controlled by varying the breakdown voltage. In the left graph of figure 7 the spectra of the source operated at 7.5 kV, 8.5 kV and 10 kV are compared. The intensity distribution inside the spectrum shifts to the left for a reduced breakdown voltage as well as the edge from which significant radiation is detectable. While for 10 kV the spectrum already starts at ~6nm the first detectable lines for 7.5 kV are at 8nm. When applying these measures, higher diffraction order interaction is not to be expected in the wavelength range below 16nm. If especially higher wavelength ranges are of interest for measurements, additional spectral filters can be used to suppress radiation from smaller wavelengths (see figure 7 right).

Straylight

Straylight is another factor which must be considered for the accuracy analysis. While the dark signal CCD measurements cover straylight that comes from steady sources, the EUV source itself gives also rise to straylight. Some part of the radiation is scattered off the optical components and captured by the CCD cameras. Distinguishing the straylight from the signal is not a trivial task. Still, an estimation on the straylight can be given by analyzing the signal on the cameras in the lower spectral range, where no direct radiation from the source is expected. In the left graph of figure 7, straylight on the CCD camera can be distinguished as a signal of 1000 to 10000 counts per pixel, depending on the breakdown voltage. Even in the spectral range above 10nm, where the intensity of the spectrum is high, the straylight can make up 1% to 10% of the signal. By measuring the straylight in the spectral range below 6nm it can be distracted from the signal to reduce the systematical error on the measurement. Still an unknown error can remain as the distribution of the straylight over the camera does not have to be uniform.

To gain more information on the uniformity of the straylight an additional measurement of the whole spectrum is done in with and without an additional spectral filter of silicon-rich nitride with a thickness of 200nm

(figure 7 right). This filter suppresses radiation from below 10nm. The straylight per pixel for both measurements can be estimated by averaging the signal below 8nm for the non-filtered measurement and below 10nm for the filtered measurement.

A finding of this work is, that the ratio between straylight per pixel and the integrated intensity of the whole detectable spectral range is almost identical for both measurements. The value was determined to be $2.41 \cdot 10^{-5}$ for the non-filtered measurement and $2.39 \cdot 10^{-5}$ for the filtered measurement. This is a first indication, that the straylight might be uniformly distributed over the CCD camera. Additionally, it is an indication, that the spectral distribution of the radiation the straylight might also be uniform. Both these finding give more confidence in the assumption, that a uniform correction term is acceptable to reduce the systematical errors induced by straylight.

3.2 Measurement parameters

The reflectance of a sample is measured in dependency on two measurement parameters, the incidence angle on the sample and the wavelength.

Incidence angle

The statistical error of the incidence angle is already covered in the statistical error of the reflectance measurement as it is mainly attributed to the positional fluctuations of the plasma pinch. During alignment of the setup it is possible to generate an initial offset on the incidence angle, which can be determined to be in the range of 0° to 0.05°. When reconstructing sample parameters by the fitting process, this offset is an additional parameter to be determined.

Wavelength

The pixel width of the CCD cameras of 13.5μm corresponds to a width of approximately 5pm in the spectral range. Combined with the width of the entrance slit, the spectral resolution is about 0.05nm. During the assignment of wavelength values to the pixels, an upper limit for systematical offsets can be assumed to be below 10pm. When reconstructing sample parameters, the influence of these wavelength offsets is negligible. On the other hand, the spectral resolution has to be considered within the model for simulations during the reconstruction of sample parameter.

4. Reconstruction Accuracy

The reconstruction of sample parameters by fitting model data to the measured reflectance data yields results within an uncertainty that is dependent on three main factors. The first factor is the experimental uncertainty of the measurement data which was analyzed in the previous chapter. The second factor is the amount of data, meaning the number of meaningful data points, which are considered during the fitting process. Additionally, the sensitivity of the measured data to the reconstructed parameters is crucial for reconstruction. The sensitivity expresses how much the reflectance changes when varying the respective parameter[13]. The third main factor is the model accuracy. It includes deviations of the model from physical reality. These deviations are induced by the parametrization of the sample, where parameters are be simplified and neglected or fixed with assumed values.

This work focuses mainly on how the first two factors, the experimental accuracy and the number of meaningful datapoints, affect the sample parameter reconstruction. To do so, synthetic reflectance data is generated and assigned with a synthetic measurement uncertainty according to the experimental accuracy of the EUV spectrometer. The synthetic measurement data is simulated using the same model also used during fitting in order to avoid effects induced by the model accuracy. Investigations on the model accuracy and its influence on the reconstruction accuracy are left for future work.

For this study the reconstruction of optical constants of several materials at 13.5nm wavelength is selected as an exemplary application of EUV spectrometry. The samples are modeled to consist of a 40nm layer of the investigated material on a silicon substrate leaving only two free parameters for reconstruction: the refractive index n and the extinction coefficient k. The optical constants are taken from the CXRO database[14]. As the wavelength is fixed for this investigation, the only measurement parameter with influence on the amount of data is the incidence angle θ.

To get a standard for comparison, the reflectance of a sample with a 40nm layer of tantalum is simulated with an assumed relative experimental uncertainty of 2% on the reflectance data. This corresponds to the experimental accuracy of the reflectance measurements with the EUV spectrometer. The amount of data is given by the angular range of 5° to 15° in steps of 1°, which also corresponds to the current angular measurement range of the EUV spectrometer.

The synthetic measurement data is shown in the left graph of figure 8 as well as a curve of simulated data fitted to the experimental data. To estimate the agreement between measured data and simulations for various combinations of n and k the χ^2 per degree of freedom (χ^2/dof) is calculated and plotted in figure 8 on the right. The 1σ- and 3σ-confidence interval is indicated by a blue and red line respectively, the n&k values for the best fit are indicated by a black dot. The influence on the reconstruction accuracy is then calculated at location of the best fit based on the inverse covariance matrix resulting in an absolute uncertainty of 0.0023 on n and 0.0054 on k for the given example.

To investigate the influence of the measurement conditions of the EUV spectrometer synthetic alterations are conducted. One alteration is done to the experimental uncertainty changing it from 2% to 1% and 0.1%. Another alteration is done to the amount of data points, by varying the range of incidence angles, from 5° to 15° to 5° to 30°. In figure 9 the χ^2/dof plots of all combinations of the different experimental uncertainties and incidence angle ranges are shown. The confidence intervals shrink both for increasing the experimental uncertainty as well for increasing the angular range.

The resulting uncertainty on n and k are shown in figure 10. Here, the angular range is increased in steps of 1° starting from 5° to 7° and going up to 5° to 30°. From the plots can be figured, that the reconstruction uncertainty of the optical constants scales about linearly with the experimental uncertainty, as reducing the experimental uncertainty by a factor two or by an order of magnitude, does inflict the same effect on the reconstruction uncertainty. Both plots in figure 10 indicate that the angular range of reflectance measurements has a crucial impact on the reconstruction accuracy. Over the whole width of angular ranges, indicated by their maximal grazing incidence angles, the reconstruction uncertainty of the optical constants drops by approximately two orders of magnitude. The curves for the uncertainty on n and k show slightly different behavior, which indicates the different sensitivity of the measurement data for n and k. One prominent behavior is that the uncertainty on n stops decreasing for a maximum grazing angle of around 24° and for k at around 27°. This indicates that data measured at higher grazing angles is not sensitive to the optical constants anymore. This is also supported by the fact that the reflectance of tantalum tends to vanish around these grazing incidence angles (see the left graph in figure 8).

The influence on the angular range is dependent on the material under investigation. Samples of tantalum, platinum and silicon dioxide are compared in the left plot of figure 11 and it is visible that the reflectance of these three materials drop below 1% at different angular ranges. The reconstruction uncertainty on n is for the different materials in figure 11 on the right shows different behavior according to their reflectance. The reconstruction of n for silicon dioxide gives already small uncertainties for small angular ranges but measurements at incidence angles above 15° are not sensitive to n. On the other hand, the uncertainty on measurements with platinum samples is at least one order of magnitude larger compared to tantalum or silicon dioxide, but as the reflectance of platinum does not drop to zero at an incidence angle below 30°, bigger angular ranges still provide improvements to the reconstruction accuracy. By increasing the angular range to 5° to 30° a decrease on the reconstruction uncertainty of n of around one order of magnitude is achieved compared to measurements within the range of 5° to 15°.

5. Conclusion

An accuracy analysis has been conducted for a stand-alone EUV spectrometer used for characterization of samples relevant for the semiconductor industry. In benchmarking experiments the experimental uncertainty is determined to be ~2% within the spectral range of 10.5nm to 14nm. The uncertainty is mainly influenced by systematical errors, while the statistical errors of the reflectance measurements only amount to ~0.15%. The major systematical error of the setup is induced by the thermal instability of the in-vacuum CCD camera and amounts to ~1%. In future work it will be addressed by the installation of a vacuum-compatible cooling system. Other systematical errors were identified and approaches to decrease them in future works were presented.

Systematical errors with distinguishable influence on the reflectance like an offset on the incidence angle are separated from the experimental uncertainty of the measurement. During parameter reconstruction they are treated as additional fitting parameters. Another finding is that, while most systematical errors are negligible in the spectral range of 10.5nm to 14nm, they gain a significant influence when expanding the spectral range.

The impact of the experimental conditions in the EUV spectrometer with respect to the characterization of optical constants of an ultrathin film layer sample has been investigated. The influence of the experimental uncertainty on the reconstruction accuracy of the optical contents is determined to be approximately linear. The influence of the angular range is dependent on the investigated material and its reflectance. Using data of a broader angular range for the parameter reconstruction decreases the reconstruction uncertainty as long as the reflectance at the included grazing incidence angles does not vanish. This investigation demonstrates that an increase of the angular range of measurements from 5° to 15° to 5° to 30° can decrease the reconstruction uncertainty significantly by around one order of magnitude.

In future works, the angular range of the EUV spectrometer will be increased to grazing incidence angles up to 30° to increase the amount of collectible data. Further, the remaining systematical error on measurements in this wider angular range and a wider spectral range are going to be investigated. Additional measures to enhance the accuracy of measurements with the EUV spectrometer are going to be identified.

6. Acknowledgements

This project has received funding from DFG - Deutsche Forschungsgemeinschaft under project number 415848294 - "Spectroscopic EUV metrology for nanoscale gratings" (GZ: LO 640/27-1). This project also has received funding from the Electronic Component Systems for European Leadership Undertaking under grant agreement number 783247. This Joint Undertaking receives support from the European Union's Horizon 2020 research and innovation programme and Netherlands, France, Belgium, Germany, Czech Republic, Austria, Hungary, Israel. Additionally, this project has received funding from the German Federal Ministry for Economic Affairs and Energy (BMWi) (ZF4109603SY9). The authors also acknowledge Victor Soltwisch (PTB) for the synchrotron measurements.

7. References

[1] IEEE, "International Roadmap for Devices and Systems 2020 Edition Metrology," IEEE 2020.

[2] Bunday, B., Solecky, E., Vaid, A., Bello, A. F., and Dai, X., "Metrology capabilities and needs for 7nm and 5nm logic nodes," **Proc. SPIE 101450G** (2017).

[3] Orji, N. G., Badaroglu, M., Barnes, B. M., Beitia, C., Bunday, B. D., Celano, U., Kline, R. J., Neisser, M., Obeng, Y., and Vladar, A. E., "Metrology for the next generation of semiconductor devices," *Nature electronics 1* (2018).

[4] Bahrenberg, L., Glabisch, S., Danylyuk, S., Ghafoori, M., Schroeder, S., Brose, S., Stollenwerk, J., and Loosen, P., "Nanoscale grating characterization through EUV spectroscopy aided by machine learning techniques," **Proc. SPIE 11325**, 113250X (2020).

[5] Bahrenberg, L., Glabisch, S., Ghafoori, M., Brose, S., Danylyuk, S., Stollenwerk, J., and Loosen, P., "Laboratory-based EUV spectroscopy for the characterization of thin films, membranes and nanostructured surfaces," **Proc. SPIE 11147**, 111471X (2019).

[6] Danylyuk, S., Herbert, S., Loosen, P., Lebert, R., Schäfer, A., Schubert, J., Tryus, M., and Juschkin, L., "Multi- Angle Spectroscopic Extreme Ultraviolet Reflectometry for Analysis of Thin Films and Interfaces," *Phys. Status Solidi C 12(3)*, 12(3) 318–322 (2015).

[7] Bahrenberg, L., Danylyuk, S., Glabisch, S., Ghafoori, M., Schröder, S., Brose, S., Stollenwerk, J., and Loosen, P., "Characterization of nanoscale gratings by spectroscopic reflectometry in the extreme ultraviolet with a standalone setup," *Opt. Express 28(14)*, 20489–20502 (2020).

[8] Bergmann, K., Schriever, G., Rosier, O., Müller, M., Neff, W., and Lebert, R., "Highly repetitive, extreme-ultraviolet radiation source based on a gas-discharge plasma," *Appl. Opt. 25(38)*, 5413–5417 (1999).

[9] JCGM, "Guide to the expression of uncertainty in measurement - JCGM 100:2008 (GUM 1995 with minor corrections - Evaluation of measurement data),".

[10] Lebert, R., Wies, C., Jaegle, B., Juschkin, L., Bieberle, U., Meisen, M., Neff, W., Bergmann, K., Walter, K., Rosier, O., Schuermann, M. C., and Missalla, T., "Status of EUV-lamp development and demonstration of applications," **Proc. SPIE 943** (2004).

[11] Janesick, J. R., [Photon transfer], SPIE, Bellingham, Wash. (1000 20th St. Bellingham WA 98225-6705 USA) (2007).

[12] Shin, H., Sporre, J. R., Raju, R., and Ruzic, D. N., "Reflectivity degradation of grazing-incident EUV mirrors by EUV exposure and carbon contamination," *Microelectronic Engineering 86(1)*, 99–105 (2009).

[13] Silver, R., Germer, T., Attota, R., Barnes, B. M., and Bunday, B., "Fundamental limits of optical critical dimension metrology: a simulation study," **Proc. SPIE 65180U** (2007).

[14] Henke, B. L., Gullikson, E. M., and Davis, J. C., "X-ray interactions: photoabsorption, scattering, transmission and reflection," *Atomic Data and Nuclear Data Tables (54)*, 181–342 (1993).

Industry Briefs

US Manufacturing Index Approaches 2-year High (EPSNews)

U.S. manufacturing in October expanded at its highest rate since 2018, driven by the strongest orders growth since 2004 and an uptick in factory employment. The Institute for Supply Management's manufacturing index, the PMI, grew 3.9 percent to 59.3 in October, while new orders increased 7.7 percent to reach 67.9.

https://epsnews.com/2020/11/02/u-s-manufacturing-index-approaches-2-year-high/

300mm Fab Spend Skyrocketing: 38 New Fabs Expected by 2024 (Tom's Hardware)

Demand for advanced chips has been increasing gradually in the recent years and is expected to snowball faster in the coming years, due to trends like 5G, artificial intelligence, high-performance computing and edge computing. A report from SEMI, an association of chip design and manufacturing supply chain companies, predicts that at least 38 new 300mm fabs will come online by 2024, significantly increasing available capacity.

https://www.tomshardware.com/news/300mm-fab-spend-skyrocketing-38-new-fabs-expected-by-2024

Mask/Lithography Issues for Mature Nodes (Semiconductor Engineering)

Experts at the Table: Spare parts are scarce for some tools and they don't do everything, but they are nearly free to operate. That limits purchases of new equipment. Semiconductor Engineering sat down to discuss lithography and photomask issues with Bryan Kasprowicz, director of technology and strategy and a distinguished member of the technical staff at Photronics, Harry Levinson, principal at HJL Lithography, Noriaki Nakayamada, senior technologist at NuFlare, and Aki Fujimura, chief executive of D2S. What follows are excerpts of that conversation.

https://semiengineering.com/mask-lithography-issues-for-mature-nodes/

The Future of Semiconductor Manufacturing, by Syed Alam (Accenture) (EE Times/DesignLines)

While internal manufacturing made sense in the earlier days of the industry, consolidation and speed-to-market success in foundries have enabled leading semiconductor companies to compete successfully without their own manufacturing fabs. Most semiconductor companies nowadays do not have their own fabs — and they don't need to. Foundries provide the scale, breadth and diversity needed. In fact, even non-semiconductor companies such as Facebook, Amazon and Apple are now taking advantage of the fabless model to design their own chips and integrate vertically. The continued emergence of opportunities for semiconductors such as 5G, the Internet of Things (IoT) and autonomous driving, along with the proven success of the foundry model, are driving semiconductor companies to reconsider their growth and manufacturing strategies.

https://www.eetimes.com/the-future-of-semiconductor-manufacturing/?utm_source=newsletter&utm_campaign=link&utm_medium=EETimesDaily-20201106&oly_enc_id=3469J6065934A5X#

Join the premier professional organization for mask makers and mask users!

About the BACUS Group

Founded in 1980 by a group of chrome blank users wanting a single voice to interact with suppliers, BACUS has grown to become the largest and most widely known forum for the exchange of technical information of interest to photomask and reticle makers. BACUS joined SPIE in January of 1991 to expand the exchange of information with mask makers around the world.

The group sponsors an informative monthly meeting and newsletter, BACUS News. The BACUS annual Photomask Technology Symposium covers photomask technology, photomask processes, lithography, materials and resists, phase shift masks, inspection and repair, metrology, and quality and manufacturing management.

Individual Membership Benefits include:

- Subscription to BACUS News (monthly)
- Eligibility to hold office on BACUS Steering Committee

spie.org/bacushome

Corporate Membership Benefits include:

- 3-10 Voting Members in the SPIE General Membership, depending on tier level
- Subscription to BACUS News (monthly)
- One online SPIE Journal Subscription
- Listed as a Corporate Member in the BACUS Monthly Newsletter

spie.org/bacushome

CALENDAR

2021

SPIE Advanced Lithography
21-25 February 2021
San Jose, California, USA
www.spie.org/al

Photomask Japan
20-22 April 2021
Digital Forum
Japan
www.photomask-japan.org

The 36th European Mask and Lithography Conference, EMLC 2021
21-23 June 2021
Leuven, Belgium
www.emlc-conference.com/en

SPIE Photomask Technology + EUV Lithography
26-29 September 2021
www.spie.org/conferences-and-exhibitions/photomask-technology--extreme-ultraviolet-lithography

SPIE is the international society for optics and photonics, an educational not-for-profit organization founded in 1955 to advance light-based science and technology. The Society serves more than 255,000 constituents from 183 countries, offering conferences and their published proceedings, continuing education, books, journals, and the SPIE Digital Library in support of interdisciplinary information exchange, professional networking, and patent precedent. In 2019, SPIE provided more than $5 million in community support including scholarships and awards, outreach and advocacy programs, travel grants, public policy, and educational resources. **spie.org**

SPIE.
International Headquarters
P.O. Box 10, Bellingham, WA 98227-0010 USA
Tel: +1 360 676 3290
Fax: +1 360 647 1445
help@spie.org • **spie.org**

Shipping Address
1000 20th St., Bellingham, WA 98225-6705 USA

Managed by SPIE Europe
2 Alexandra Gate, Ffordd Pengam, Cardiff,
CF24 2SA, UK
Tel: +44 29 2089 4747
Fax: +44 29 2089 4750
spieeurope@spieeurope.org • **spieeurope.org**

You are invited to submit events of interest for this calendar. Please send to lindad@spie.org.